

A Chemically Doped Naphthalenediimide-Bithiazole Polymer for n-Type Organic Thermoelectrics

Suhao Wang, Hengda Sun, Tim Erdmann, Gang Wang, Daniele Fazzi, Uwe Lappan, Yuttapoom Puttisong, Zhihua Chen, Magnus Berggren, Xavier Crispin, Anton Kiriy, Brigitte Voit, Tobin J. Marks, Simone Fabiano and Antonio Facchetti

The self-archived postprint version of this journal article is available at Linköping University Institutional Repository (DiVA):

<http://urn.kb.se/resolve?urn=urn:nbn:se:liu:diva-151506>

N.B.: When citing this work, cite the original publication.

Wang, S., Sun, H., Erdmann, T., Wang, G., Fazzi, D., Lappan, U., Puttisong, Y., Chen, Z., Berggren, M., Crispin, X., Kiriy, A., Voit, B., Marks, T. J., Fabiano, S., Facchetti, A., (2018), A Chemically Doped Naphthalenediimide-Bithiazole Polymer for n-Type Organic Thermoelectrics, *Advanced Materials*, 30(31), 1801898. <https://doi.org/10.1002/adma.201801898>

Original publication available at:

<https://doi.org/10.1002/adma.201801898>

Copyright: Wiley (12 months)

<http://eu.wiley.com/WileyCDA/>



DOI: 10.1002/((please add manuscript number))

Article type: Communication

A chemically doped naphthalenediimide–bithiazole polymer for n-type organic thermoelectrics

Suhao Wang, Hengda Sun, Tim Erdmann, Gang Wang, Daniele Fazzi, Uwe Lappan, Yuttapoom Puttisong, Zhihua Chen, Magnus Berggren, Xavier Crispin, Anton Kiriy, Brigitte Voit, Tobin J. Marks, Simone Fabiano,* Antonio Facchetti**

Dr. S. Wang, Dr. H. Sun, Prof. M. Berggren, Prof. X. Crispin, Dr. S. Fabiano
Laboratory of Organic Electronics, Department of Science and Technology, Linköping
University, SE-601 74 Norrköping, Sweden
E-mail: simone.fabiano@liu.se

Dr. T. Erdmann,^[+] Dr. A. Kiriy, Prof. B. Voit
Technische Universität Dresden, Center for Advancing Electronics Dresden, D-01062 Dresden,
Germany
^[+]Present address: IBM Almaden Research Center, 650 Harry Road, San Jose, CA95120, USA

Dr. T. Erdmann, Dr. U. Lappan, Dr. A. Kiriy, Prof. B. Voit
Leibniz-Institut für Polymerforschung Dresden e.V., D-010 69 Dresden, Germany

Dr. T. Erdmann, Dr. Z. Chen, Dr. S. Fabiano, Prof. A. Facchetti
Flexterra Corporation, 8025 Lamon Avenue, Skokie, Illinois 60077, USA
E-mail: afacchetti@flexterracorp.com

Dr. G. Wang, Prof. T. J. Marks, Dr. S. Fabiano, Prof. A. Facchetti
Department of Chemistry and the Materials Research Center, Northwestern University, 2145
Sheridan Road, Evanston, Illinois 60208, USA
E-mail: t-marks@northwestern.edu

Dr. D. Fazzi^[++]
Max-Planck-Institut für Kohlenforschung Kaiser-Wilhelm-Platz 1, D-45470 Mülheim an der
Ruhr, Germany
^[++]Present address: Institut für Physikalische Chemie, Department Chemie, Universität zu Köln
Luxemburger Str. 116D-50939 Köln

Dr. Y. Puttisong
Department of Physics, Chemistry and Biology, Linköping University, SE-581 83 Linköping,
Sweden

Keywords: donor-acceptor polymers, doping, polymers, n-type polymers, organic thermoelectrics

The synthesis of a novel naphthalenediimide (NDI)-bithiazole (Tz2)-based polymer [P(NDI2OD-Tz2)] is reported and structural, thin-film morphological, as well as charge transport and thermoelectric properties are compared to the parent and widely investigated NDI-bithiophene (T2) polymer [P(NDI2OD-T2)]. Since the steric repulsions in Tz2 are far lower than in T2, P(NDI2OD-Tz2) exhibits a more planar and rigid backbone, enhancing π - π chain stacking and intermolecular interactions. In addition, the electron-deficient nature of Tz2 enhances polymer electron affinity, thus reducing the polymer donor-acceptor character. When n-doped with amines, P(NDI2OD-Tz2) achieves electrical conductivity ($\approx 0.1 \text{ S cm}^{-1}$) and a power factor ($1.5 \mu\text{W m}^{-1} \text{ K}^{-2}$) far greater than those of P(NDI2OD-T2) (0.003 S cm^{-1} and $0.012 \mu\text{W m}^{-1} \text{ K}^{-2}$, respectively). These results demonstrate that planarized NDI-based polymers with reduced donor-acceptor character can achieve substantial electrical conductivity and thermoelectric response.

π -Conjugated polymers are emerging semiconductors for applications in printed opto-electronic, solid-state energy conversion, and energy storage devices.^[1] The conductivity of several conjugated polymers can be enhanced by molecular doping,^[2] achieved by either oxidizing (p-doping) or reducing (n-doping) the π -conjugated (macro)molecular host with a guest dopant. Doping can then reduce the injection/extraction barriers, minimizing ohmic losses in organic light-emitting diodes (OLEDs),^[3] organic photovoltaics (OPVs),^[4] and organic field-effect transistors (OFETs),^[5] as well as maximize the power factor, thus the heat-to-electricity conversion efficiency of emerging organic thermoelectric materials.^[6]

Several electronic devices require both p-type (hole-transporting) and n-type (electron-transporting) semiconductors. Although p-type polymers can efficiently be doped and exhibit exceptionally high electrical conductivity (σ) values $>1000 \text{ S cm}^{-1}$,^[7] n-doped polymer

conductivity is far lower. Recently, several air-stable n-type semiconducting polymers have been reported, particularly in the OFET/OPV literature.^[8] However, those exhibiting high electron conductivities are limited, e.g., halo-substituted benzodifurandione-phenylvinylene polymers ($\sigma = 0.6\text{-}14\text{ S/cm}$),^[9] while most polymers are limited to $\sigma < 0.01\text{ S cm}^{-1}$. For example, the donor-acceptor naphthalenediimide-bithiophene P(NDI2OD-T2) polymer (**Figure 1A**)^[10] can be doped with rhodocene,^[11] dimethylbenzimidazoline-derivatives (DMBI),^[12] amines such as polyethylenimine,^[13] or tetrakis(dimethylamino)ethylene (TDAE),^[14] and with even more strongly n-doping DMBI dimers^[15] achieving only a modest σ of $\approx 0.002\text{-}0.004\text{ S cm}^{-1}$. This result is ascribable to a strong charge carrier intra-chain localization,^[16] typical of donor-acceptor polymers.^[17] The use of highly-planarized ladder-type polymers such as poly(benzobisimidazobenzophenanthroline) (BBL, **Figure 1A**) helps overcome this limitation, reaching $\sigma \approx 1000\times$ that of backbone-distorted P(NDI2OD-T2).^[14] However, the principal limitation of BBL is marginal solubility in common organic solvents. Here we report the synthesis of the novel NDI-bithiazole-based polymer, P(NDI2OD-Tz2), and its physical, charge transport, doping, and thermoelectric properties vis-à-vis the parent P(NDI2OD-T2). The 5,5'-di(1,3-thiazolyl) (Tz2) moiety linked to the NDI core at the C-2/C-2' positions has a fewer internal steric repulsions than NDI-T2, promoting a more planar macromolecular structure. In addition, the electron-deficient nature of Tz2 enhances the electron affinity, thus reducing the polymer donor-acceptor character. The resulting polymer is more tightly packed, can be doped to a higher extent, and exhibits enhanced thermoelectric response.

Various strategies were investigated for P(NDI2OD-Tz2) synthesis, including conventional Stille polycondensation, direct arylation, and active-zinc polymerization (AZP), but only the latter protocol afforded high molecular weight (M_w) copolymers (**Figure 1B**). To utilize AZP, the new

NDI2OD-Tz2Br2 monomer was synthesized in two steps (see Supporting Information). Note that bromination of NDI2OD-Tz2 by NBS or Br₂ under neutral or strongly acidic conditions fails (Table S1), however, performing it in the presence of a weak base, pyridine, affords NDI2OD-Tz2Br2 in 61% yield. The benefit of using pyridine is two-fold. First, an in-situ formation of N-bromopyridinium bromide, which serves as a source of very strong electrophilic Br⁺, occurs. Second, pyridine neutralizes the byproduct of the reaction, i.e. HBr, which could otherwise protonate the reactant and thus reduce thiazolyl ring reactivity even further. A successful example of the use of pyridine/bromine in electrophilic aromatic substitution reactions has been reported.^[18] NDI2OD-Tz2Br2 was polymerized following the AZP procedure developed by Kiriy et al.^[19] After purification, electron paramagnetic resonance (EPR) spectroscopy confirmed the presence of radical-anion species [NDI2OD-Tz2Br2]^{•-} and indicated negative charge delocalization over both the NDI and thiazole units (Figure S1, Supporting Information). The molecular structure of P(NDI2OD-Tz2) was confirmed by high temperature proton nuclear magnetic resonance spectroscopy (¹H NMR, Figure S2, Supporting Information), and the number-average molecular mass (*M_n*) of 32.2 kDa and dispersity (*Đ*) of 1.7 by gel permeation chromatography (GPC). Thermogravimetric analysis (TGA) and differential scanning calorimetry (DSC) indicate a decomposition temperature of 412 °C (Figure S3, Supporting Information) and an endothermic/exothermic phase transition during the heating/cooling scan at 323 °C/317 °C, respectively (Figure S4, Supporting Information). Three successive heating-cooling cycles support the reversibility of this processes ($\Delta H \sim |6.9|$ J/g). Compared to P(NDI2OD-T2) with a similar *M_n* (Figure S4), P(NDI2OD-Tz2) melting and crystallization occur at 16 °C and 24 °C higher temperatures, respectively, indicating stronger intermolecular cohesion. Cyclic voltammograms of P(NDI2OD-Tz2) thin films exhibits two reversible

reductions ($E_{1/2}$) at -0.81/-1.18 V (Figure S5, Supporting Information), placing the lowest unoccupied molecular orbital (LUMO) energy at -4.10 eV from the first onset potential, which is comparable to that of P(NDI2OD-T2) (-3.99 eV). This result indicates strong LUMO localization on the naphthalenediimide portion of such NDI-based polymers.^[17] A highest occupied molecular orbital (HOMO) energy of -5.90 eV is estimated for P(NDI2OD-Tz2) from the optical band gap (E_g^{opt}) of 1.80 eV, vs. -5.46 eV for P(NDI2OD-T2) ($E_g^{\text{opt}} = 1.47$ eV).

The conformational space occupied by P(NDI2OD-Tz2) was explored by computing the potential energy profile of the NDI-Tz2 block along the dihedral angle θ connecting the two subunits (**Figure 2**; details in the Supporting Information). DFT calculations reveal a broad and flat potential profile for $\theta \approx 90^\circ$, with an absolute minimum at 80° . Co-planar conformations at $\theta = 0^\circ$ and 180° are predicted as local maxima. The rotational barrier through $\theta = 180^\circ$ (N \cdots O and S \cdots CH interactions) is 7.8 kcal/mol, thus hindering the rotation of the sub-units, while at $\theta = 0^\circ$ (N \cdots CH and S \cdots O interactions) the barrier is ≈ 0.7 kcal/mol, slightly above thermal fluctuations (≈ 0.6 kcal/mol at 298 K). Thus, the potential energy profile is essentially flat for *quasi*-planar conformations ($-20^\circ \leq \theta \leq 20^\circ$), meaning they are populated at room temperature. These data indicate that strong intermolecular interactions occurring in packed supra-molecular architectures can lead to an effective planarization of the NDI-Tz2 unit in P(NDI2OD-Tz2). The computed potential profile for NDI-Tz2 contrasts with the one of NDI-T2, where an energy barrier of ≈ 2.2 kcal mol $^{-1}$ is computed for rotation around $\theta = 0^\circ$. This highlights an intrinsic structural difference between P(NDI2OD-Tz2) and P(NDI2OD-T2), with the former having greater conformational freedom with respect to the latter.

Top-gate bottom-contact OFETs of structure Au/polymer/PMMA/Al were fabricated (see SI) to assess charge transport in the undoped polymers. P(NDI2OD-Tz2) and P(NDI2OD-T2) devices

measured in air (Figure S6, Supporting Information) have similar electron mobilities of ≈ 0.10 and $\approx 0.20 \text{ cm}^2 \text{ V}^{-1} \text{ s}^{-1}$, respectively. Next, the polymer electrical conductivity was investigated before/after film exposure to TDAE vapor for various times (t_{vapor}). **Figure 3A** indicates that P(NDI2OD-Tz2) σ is as low as $\approx 10^{-8} \text{ S cm}^{-1}$ before exposure and dramatically increases to $\approx 0.1 \text{ S cm}^{-1}$ ($\sigma_{\text{avg}} = 0.07 \pm 0.02 \text{ S cm}^{-1}$) at $t_{\text{vapor}} = \approx 16 \text{ sec}$. Remarkably, this σ is $>30\times$ larger than that measured for doped P(NDI2OD-T2) films ($\sigma_{\text{max}} = 0.003 \text{ S cm}^{-1}$), suggesting greater charge density. Quantitative EPR measurements performed on P(NDI2OD-Tz2) and P(NDI2OD-T2) films doped to their maximum conductivity values, reveals a spin density for P(NDI2OD-Tz2) of $8.65 \times 10^{20} \text{ cm}^{-3}$, which is about $35\times$ that of P(NDI2OD-T2) ($2.46 \times 10^{19} \text{ cm}^{-3}$, Figure S7A). We also measured the work function of doped P(NDI2OD-Tz2) and P(NDI2OD-T2) thin films by using Kelvin Probe (Figure S7B). For the same TDAE exposure time, doped P(NDI2OD-Tz2) films exhibit a lower work function than that of doped P(NDI2OD-T2) films, indicating increased doping levels for the former film.^[20] This result is consistent with the EPR and conductivity data. The greater conductivity of P(NDI2OD-Tz2), compared to analogous P(NDI2OD-T2) is striking considering that both polymers have similar LUMO energies and OFET electron mobilities. Thus, we believe that the superior doping efficiency in P(NDI2OD-Tz2) results from the slightly enhanced electron affinity, reduced donor-acceptor character,^[21] and the aforementioned backbone planarization. From variable-temperature conductivity measurements, the Arrhenius activation energies for charge transport are 0.20 eV and 0.30 eV for P(NDI2OD-Tz2) and P(NDI2OD-T2), respectively (Figure S8). The electrical conductivity of both doped polymers is stable under nitrogen, but it rapidly decays once the doped films are exposed to air. We attribute this result to either the susceptibility of the mobile electrons to water and/or oxygen of the ambient, which severely suppresses electron transport, or to the poor air

stability of TDAE, which is known to chemiluminesce in the presence of oxygen.^[22] To overcome the latter issue, one possible strategy is to use air-stable dopants such as tetrabutylammonium fluoride (TBAF), that has been reported to improve the air-stability of n-doped polymers.^[9b] The conductivity of P(NDI2OD-Tz2) films begins to decline for longer TDAE exposures, reaching $\sim 0.001 \text{ S cm}^{-1}$ and $< 10^{-5} \text{ S cm}^{-1}$ for t_{vapor} of 30 min and 3 h, respectively (Figure S9). We attribute this result to a disruption of the film microstructure (*vide infra*). In preliminary experiments, we have also carried out solution doping of P(NDI2OD-Tz2) by using the molecular dopant DMBI, a process which is more relevant to roll-to-roll printed electronics, affording $\sigma \approx 0.007 \text{ S cm}^{-1}$. We ascribe the lower conductivity of DMBI-solution doped films, as opposed to the TDAE-vapor doped ones, to the well-known poor miscibility of DMBI in host polymer matrixes.^[12] This extrinsic limitation may be overcome by a proper engineering of the alkyl side chains.^[20, 23] Optimization is in progress and will be reported in a successive study.

The optical properties of P(NDI2OD-Tz2) films upon TDAE exposure were investigated by UV-Vis-NIR absorption spectroscopy (Figure 3B). The spectrum of undoped P(NDI2OD-Tz2) films consists of two major features, a high-energy $\pi\text{-}\pi^*$ transition band at $\sim 363 \text{ nm}$ and a low-energy band at $\sim 588 \text{ nm}$, attributable to an intramolecular charge-transfer (CT) transition. Compared to undoped P(NDI2OD-Tz2), the absorption spectra of P(NDI2OD-Tz2) is blue-shifted, most reflecting the greater Tz2 unit electron-deficiency, which reduces the extent of CT (Figure S10A). TDAE exposure of P(NDI2OD-Tz2) films is accompanied by a sharp decrease in the band intensity at $\sim 588 \text{ nm}$, along with the rise of two new features at ~ 500 and $\sim 820 \text{ nm}$, respectively. This is accompanied by a dramatic change in the film color (Figure 3B), and in agreement with the increase in the electrical conductivity. Furthermore, the band at $\sim 363 \text{ nm}$

shifts as the n-doping level is increased (Figure S10B). The optical spectra data are consistent with the formation of negative polarons.^[14, 24]

Grazing incidence wide-angle X-ray scattering (GIWAXS) was performed to investigate doping effects on the polymer film microstructures (**Figure 4**; details in Supporting Information). The two-dimensional (2D) diffraction pattern of P(NDI2OD-Tz2) films exhibits long-range ordering originating from a mixed π -face-on and edge-on chain orientations. The π - π stacking peak along the q_z axis corresponds to a d -spacing of 3.64 Å, which is significantly smaller than that of P(NDI2OD-T2) (3.92 Å) and is consistent with the DFT-computed planarization of the polymer backbone (*vide supra*). A similar effect on the π - π staking distance has been recently reported for highly planarized NDI-bifuran polymers,^[25] and the increased planarity is also reflected in the reduced solubility of P(NDI2OD-Tz2). After ≈ 3 min exposure to the TDAE dopant, when the conductivities of both polymers reach the maximum values, both polymer films exhibit enhanced crystallinity and a more intense π - π stacking out-of-plane reflection, with d -spacings of 3.60 Å and 3.89 Å for P(NDI2OD-Tz2) and P(NDI2OD-T2), respectively (Figures S11-S12). For longer exposure times, the crystallinity of both polymers is disrupted. This result is in agreement with the morphology changes observed by atomic force microscopy (AFM, Figures S13-S14), and fully consistent with the reduction of conductivity observed in Figure S8. This observation is qualitatively similar to what is typically reported for p-doped polymers at high molar doping concentration, regardless of the doping method.^[26]

The thermoelectric properties of P(NDI2OD-Tz2) films were next investigated. The Seebeck coefficients (S) of the doped films were measured as a function of the TDAE exposure time in a N₂-filled glove box (**Figure 5A**; details in Supporting Information). Thus, S of the P(NDI2OD-Tz2) films decreases by $\sim 3\times$ upon exposure to TDAE vapors, going from $-732 \pm 31 \mu\text{V K}^{-1}$ ($\sigma \approx$

0.004 S cm⁻¹) for $t_{\text{vapor}} = 10$ sec, to $-447 \pm 15 \mu\text{V K}^{-1}$ ($\sigma \approx 0.06$ S cm⁻¹) for $t_{\text{vapor}} = 3$ min, to $-227 \pm 11 \mu\text{V K}^{-1}$ ($\sigma \approx 0.004$ S cm⁻¹) for $t_{\text{vapor}} = 1.7$ h. The negative sign of S agrees with the n-type doping of the film. Since σ and S are interrelated as a function of the charge carrier concentration, typically featuring opposite trends, the sample power factor ($\text{PF} = S^2\sigma$) should optimize at an intermediate exposure time (i.e., doping level). For P(NDI2OD-Tz2), a maximum PF of $1.5 \mu\text{W m}^{-1} \text{K}^{-2}$ is obtained for $t_{\text{vapor}} = 3$ min, which is 100× greater than that of P(NDI2OD-T2) ($0.012 \mu\text{W m}^{-1} \text{K}^{-2}$, Figure 5B). This is among the highest PF values reported to date for NDI-based n-doped polymers (see Table S2 for a literature survey of n-doped polymer thermoelectrics).^[12, 14, 27] Interestingly, note that P(NDI2OD-Tz2) follows the empirical relation of $S \propto \sigma^{-1/4}$ (Figure S15), as already observed for other semiconducting polymers,^[28] while P(NDI2OD-T2) shows a stronger dependence on σ ($S \propto \sigma^{-1/2}$).^[14] Although the origin of this empirical trend is not yet fully understood, it is typically ascribed to inhomogeneous disorder in polymer semiconductors^[29] as well as to a broadening of the density of states due to the attractive Coulomb potential of ionized dopants.^[30] For instance, early studies on stretched polyaniline films^[31] have suggested that a different dependence of S over σ may originate from variations in molecular order, as more recently observed for ladder-type polymers.^[14]

In summary, a new naphthalenediimide-bithiazole n-type semiconducting polymer was synthesized and characterized. Importantly, the reduced intrachain steric demands in Tz2 versus T2 give rise to greater backbone planarity, hence stronger intermolecular π - π stacking interactions. Furthermore, the electron-deficient nature of Tz2 enhances the electron affinity and reduces donor-acceptor character. When doped with TDAE, P(NDI2OD-Tz2) can reach an electrical conductivity and thermoelectric power factor far superior to those of analogous

P(NDI2OD-T2). Higher σ and PF might be achieved by engineering of alkyl side chains which should enhance crystallinity^[23a] and/or dopant-polymer miscibility.^[20, 23b]

Experimental Section

Detailed description and discussion of the materials synthesis and characterization, device fabrication method, electrical measurements, and DFT calculations as well as supplementary figures can be found in the Supporting Information.

Supporting Information

Supporting Information is available from the Wiley Online Library or from the author.

Acknowledgements

S.W., H.S. and T.E. contributed equally to this work. T.E. present address: IBM Almaden Research Center, 650 Harry Road, San Jose, CA 95120, USA. The authors acknowledge the Knut and Alice Wallenberg Foundation (Tail of the Sun Project) and the Swedish Foundation for Strategic Research (Synergy project), for support of this research. S.F. gratefully acknowledges funding by VINNOVA (2015-04859), the Swedish Research Council (2016-03979), and the Advanced Functional Materials Center at Linköping University (2009-00971). G.W. was supported by award 70NANB14H012 from the U.S. Department of Commerce, National Institute of Standards and Technology as part of the Center for Hierarchical Materials Design (CHiMaD). This research used resources of the Advanced Photon Source, a U.S. Department of Energy (DOE) office of Science User Facility operated for the DOE Office of Science by Argonne National Laboratory under Contract No. DE-AC02-06CH11357. This work was partly supported by DFG within the CoEcaed and grant KI-1094/9 (A.K.) as well as the Humboldt Foundation (T.E.). T.E. thanks H. Komber, L. Häußler, and K. Arnhold for helpful discussions.

Received: ((will be filled in by the editorial staff))

Revised: ((will be filled in by the editorial staff))

Published online: ((will be filled in by the editorial staff))

References

- [1] a) L. Zhang, Y. Cao, N. S. Colella, Y. Liang, J.-L. Brédas, K. N. Houk, A. L. Briseno, *Acc. Chem. Res.* **2015**, *48*, 500; b) A. C. Arias, J. D. MacKenzie, I. McCulloch, J. Rivnay, A. Salleo, *Chem. Rev.* **2010**, *110*, 3; c) A. Facchetti, *Chem. Mater.* **2011**, *23*, 733; d) H. N. Tsao, D. M. Cho, I. Park, M. R. Hansen, A. Mavrinskiy, D. Y. Yoon, R. Graf, W. Pisula, H. W. Spiess, K. Müllen, *J. Am. Chem. Soc.* **2011**, *133*, 2605; e) I. McCulloch, R. S. Ashraf, L. Biniek, H. Bronstein, C. Combe, J. E. Donaghey, D. I. James, C. B. Nielsen, B. C. Schroeder, W. M. Zhang, *Acc. Chem. Res.* **2012**, *45*, 714.
- [2] B. Lüssem, M. Riede, K. Leo, *Phys. Status Solidi A* **2013**, *210*, 9.
- [3] a) P. Zalar, Z. B. Henson, G. C. Welch, G. C. Bazan, T.-Q. Nguyen, *Angew. Chem. Int. Ed* **2012**, *51*, 7495; b) C. G. Tang, M. C. Y. Ang, K.-K. Choo, V. Keerthi, J.-K. Tan, M. N. Syafiqah, T. Kugler, J. H. Burroughes, R.-Q. Png, L.-L. Chua, P. K. H. Ho, *Nature* **2016**, *539*, 536.
- [4] a) Y. Zhang, H. Zhou, J. Seifert, L. Ying, A. Mikhailovsky, A. J. Heeger, G. C. Bazan, T.-Q. Nguyen, *Adv. Mater.* **2013**, *25*, 7038; b) Y. H. Zhou, C. Fuentes-Hernandez, J. Shim, J. Meyer, A. J. Giordano, H. Li, P. Winget, T. Papadopoulos, H. Cheun, J. Kim, M. Fenoll, A. Dindar, W. Haske, E. Najafabadi, T. M. Khan, H. Sojoudi, S. Barlow, S. Graham, J. L. Bredas, S. R. Marder, A. Kahn, B. Kippelen, *Science* **2012**, *336*, 327.
- [5] a) G. Lu, J. Blakesley, S. Himmelberger, P. Pingel, J. Frisch, I. Lieberwirth, I. Salzmann, M. Oehzelt, R. Di Pietro, A. Salleo, N. Koch, D. Neher, *Nat. Commun.* **2013**, *4*, 1588; b) D. Khim, K.-J. Baeg, M. Caironi, C. Liu, Y. Xu, D.-Y. Kim, Y.-Y. Noh, *Adv. Funct. Mater.* **2014**, *24*, 6252.
- [6] a) O. Bubnova, Z. U. Khan, A. Malti, S. Braun, M. Fahlman, M. Berggren, X. Crispin, *Nat. Mater.* **2011**, *10*, 429; b) R. Kroon, D. A. Mengistie, D. Kiefer, J. Hynynen, J. D. Ryan, L. Yu, C. Müller, *Chem. Soc. Rev.* **2016**, *45*, 6147; c) I. Petsagkourakis, E. Pavlopoulou, E. Cloutet, Y. F. Chen, X. Liu, M. Fahlman, M. Berggren, X. Crispin, S. Dilhaire, G. Fleury, G. Hadziioannou, *Org. Electron.* **2018**, *52*, 335.
- [7] a) C. Y. Kao, B. Lee, L. S. Wielunski, M. Heeney, I. McCulloch, E. Garfunkel, L. C. Feldman, V. Podzorov, *Adv. Funct. Mater.* **2009**, *19*, 1906; b) O. Bubnova, Z. U. Khan, H. Wang, S. Braun, D. R. Evans, M. Fabretto, P. Hojati-Talemi, D. Dagnelund, J.-B. Arlin, Y. H. Geerts, S. Desbief, D. W. Breiby, J. W. Andreasen, R. Lazzaroni, W. M. Chen, I. Zozoulenko, M. Fahlman, P. J. Murphy, M. Berggren, X. Crispin, *Nat. Mater.* **2014**, *13*, 190; c) Y. Karpov, T. Erdmann, I. Raguzin, M. Al-Hussein, M. Binner, U. Lappan, M. Stamm, K. L. Gerasimov, T. Beryozkina, V. Bakulev, D. V. Anokhin, D. A. Ivanov, F. Günther, S. Gemming, G. Seifert, B. Voit, R. Di Pietro, A. Kiriy, *Adv. Mater.* **2016**, *28*, 6003; d) S. N. Patel, A. M. Glauddell, K. A. Peterson, E. M. Thomas, K. A. O'Hara, E. Lim, M. L. Chabiny, *Sci. Adv.* **2017**, *3*, e1700434.
- [8] a) X. Zhan, A. Facchetti, S. Barlow, T. J. Marks, M. A. Ratner, M. R. Wasielewski, S. R. Marder, *Adv. Mater.* **2011**, *23*, 268; b) B. J. Jung, N. J. Tremblay, M.-L. Yeh, H. E. Katz, *Chem. Mater.* **2011**, *23*, 568.
- [9] a) K. Shi, F. Zhang, C.-A. Di, T.-W. Yan, Y. Zou, X. Zhou, D. Zhu, J.-Y. Wang, J. Pei, *J. Am. Chem. Soc.* **2015**, *137*, 6979; b) X. Zhao, D. Madan, Y. Cheng, J. Zhou, H. Li, S. M. Thon, A. E. Bragg, M. E. DeCoster, P. E. Hopkins, H. E. Katz, *Adv. Mater.* **2017**, *29*, 1606928.
- [10] a) H. Yan, Z. Chen, Y. Zheng, C. Newman, J. R. Quinn, F. Dötz, M. Kastler, A. Facchetti, *Nature* **2009**, *457*, 679; b) S. Wang, S. Fabiano, S. Himmelberger, S. Puzinas, X. Crispin, A. Salleo, M. Berggren, *Proc. Natl. Acad. Sci. U.S.A.* **2015**, *112*, 10599; c) R. Matsidik, H. Komber, A. Luzio, M. Caironi, M. Sommer, *J. Am. Chem. Soc.* **2015**, *137*, 6705; d) G. Wang, W. Huang, N. D. Eastham, S. Fabiano, E. F. Manley, L. Zeng, B. Wang, X. Zhang, Z. Chen, R.

- Li, R. P. H. Chang, L. X. Chen, M. J. Bedzyk, F. S. Melkonyan, A. Facchetti, T. J. Marks, *Proc. Natl. Acad. Sci. U.S.A.* **2017**, *114*, E10066; e) G. Wang, N. Persson, P.-H. Chu, N. Kleinhenz, B. Fu, M. Chang, N. Deb, Y. Mao, H. Wang, M. A. Grover, E. Reichmanis, *ACS Nano* **2015**, *9*, 8220.
- [11] Y. B. Qi, S. K. Mohapatra, S. B. Kim, S. Barlow, S. R. Marder, A. Kahn, *Appl. Phys. Lett.* **2012**, *100*, 4.
- [12] R. A. Schlitz, F. G. Brunetti, A. M. Glaudell, P. L. Miller, M. A. Brady, C. J. Takacs, C. J. Hawker, M. L. Chabiny, *Adv. Mater.* **2014**, *26*, 2825.
- [13] S. Fabiano, S. Braun, X. Liu, E. Weverberghs, P. Gerbaux, M. Fahlman, M. Berggren, X. Crispin, *Adv. Mater.* **2014**, *26*, 6000.
- [14] S. Wang, H. Sun, U. Ail, M. Vagin, P. O. Å. Persson, J. W. Andreasen, W. Thiel, M. Berggren, X. Crispin, D. Fazzi, S. Fabiano, *Adv. Mater.* **2016**, *28*, 10764.
- [15] B. D. Naab, S. Zhang, K. Vandewal, A. Salleo, S. Barlow, S. R. Marder, Z. Bao, *Adv. Mater.* **2014**, *26*, 4268.
- [16] B. D. Naab, X. Gu, T. Kurosawa, J. W. F. To, A. Salleo, Z. Bao, *Adv. Electron. Mater.* **2016**, *2*, 1600004.
- [17] a) D. Fazzi, M. Caironi, C. Castiglioni, *J. Am. Chem. Soc.* **2011**, *133*, 19056; b) G. Wetzelaer, M. Kuik, Y. Olivier, V. Lemaur, J. Cornil, S. Fabiano, M. A. Loi, P. W. M. Blom, *Phys. Rev. B* **2012**, *86*, 165203; c) L. Zhang, B. D. Rose, Y. Liu, M. M. Nahid, E. Gann, J. Ly, W. Zhao, S. J. Rosa, T. P. Russell, A. Facchetti, C. R. McNeill, J.-L. Brédas, A. L. Briseno, *Chem. Mater.* **2016**, *28*, 8580; d) B. J. Eckstein, F. S. Melkonyan, E. F. Manley, S. Fabiano, A. R. Mouat, L. X. Chen, A. Facchetti, T. J. Marks, *J. Am. Chem. Soc.* **2017**, *139*, 14356.
- [18] V. Benin, A. T. Yeates, D. Dudis, *J. Heterocycl. Chem.* **2008**, *45*, 811.
- [19] a) V. Senkovskyy, R. Tkachov, H. Komber, M. Sommer, M. Heuken, B. Voit, W. T. S. Huck, V. Kataev, A. Petr, A. Kiriya, *J. Am. Chem. Soc.* **2011**, *133*, 19966; b) V. Senkovskyy, R. Tkachov, H. Komber, A. John, J.-U. Sommer, A. Kiriya, *Macromolecules* **2012**, *45*, 7770; c) R. Tkachov, H. Komber, S. Rauch, A. Lederer, U. Oertel, L. Häußler, B. Voit, A. Kiriya, *Macromolecules* **2014**, *47*, 4994.
- [20] J. Liu, L. Qiu, R. Alessandri, X. Qiu, G. Portale, J. Dong, W. Talsma, G. Ye, A. A. Sengrigan, P. C. T. Souza, M. A. Loi, R. C. Chiechi, S. J. Marrink, J. C. Hummelen, L. J. A. Koster, *Adv. Mater.* **2018**, *30*, 1704630.
- [21] D. Di Nuzzo, C. Fontanesi, R. Jones, S. Allard, I. Dumsch, U. Scherf, E. von Hauff, S. Schumacher, E. Da Como, *Nat. Commun.* **2015**, *6*.
- [22] H. E. Winberg, J. E. Carnahan, D. D. Coffman, M. Brown, *J. Am. Chem. Soc.* **1965**, *87*, 2055.
- [23] a) Y. Wang, M. Nakano, T. Michinobu, Y. Kiyota, T. Mori, K. Takimiya, *Macromolecules* **2017**, *50*, 857; b) D. Kiefer, A. Giovannitti, H. Sun, T. Biskup, A. Hofmann, M. Koopmans, C. Cendra, S. Weber, L. J. Anton Koster, E. Olsson, J. Rivnay, S. Fabiano, I. McCulloch, C. Müller, *ACS Energy Lett.* **2018**, *3*, 278.
- [24] M. Caironi, M. Bird, D. Fazzi, Z. H. Chen, R. Di Pietro, C. Newman, A. Facchetti, H. Sirringhaus, *Adv. Funct. Mater.* **2011**, *21*, 3371.
- [25] R. Matsidik, A. Luzio, Ö. Askin, D. Fazzi, A. Sepe, U. Steiner, H. Komber, M. Caironi, M. Sommer, *Chem. Mater.* **2017**, *29*, 5473.
- [26] a) D. T. Duong, C. Wang, E. Antono, M. F. Toney, A. Salleo, *Org. Electron.* **2013**, *14*, 1330; b) J. Hynynen, D. Kiefer, L. Yu, R. Kroon, R. Munir, A. Amassian, M. Kemerink, C. Müller, *Macromolecules* **2017**, *50*, 8140.

- [27] D. Madan, X. Zhao, R. M. Ireland, D. Xiao, H. E. Katz, *APL Materials* **2017**, *5*, 086106.
 [28] A. M. Glaudell, J. E. Cochran, S. N. Patel, M. L. Chabynyc, *Adv. Energy Mater.* **2015**, *5*, 1401072.
 [29] S. D. Kang, G. J. Snyder, *Nature Materials* **2016**, *16*, 252.
 [30] H. Abdalla, G. Zuo, M. Kemerink, *Phys. Rev. B* **2017**, *96*, 241202.
 [31] N. Mateeva, H. Niculescu, J. Schlenoff, L. R. Testardi, *J. Appl. Phys.* **1998**, *83*, 3111.

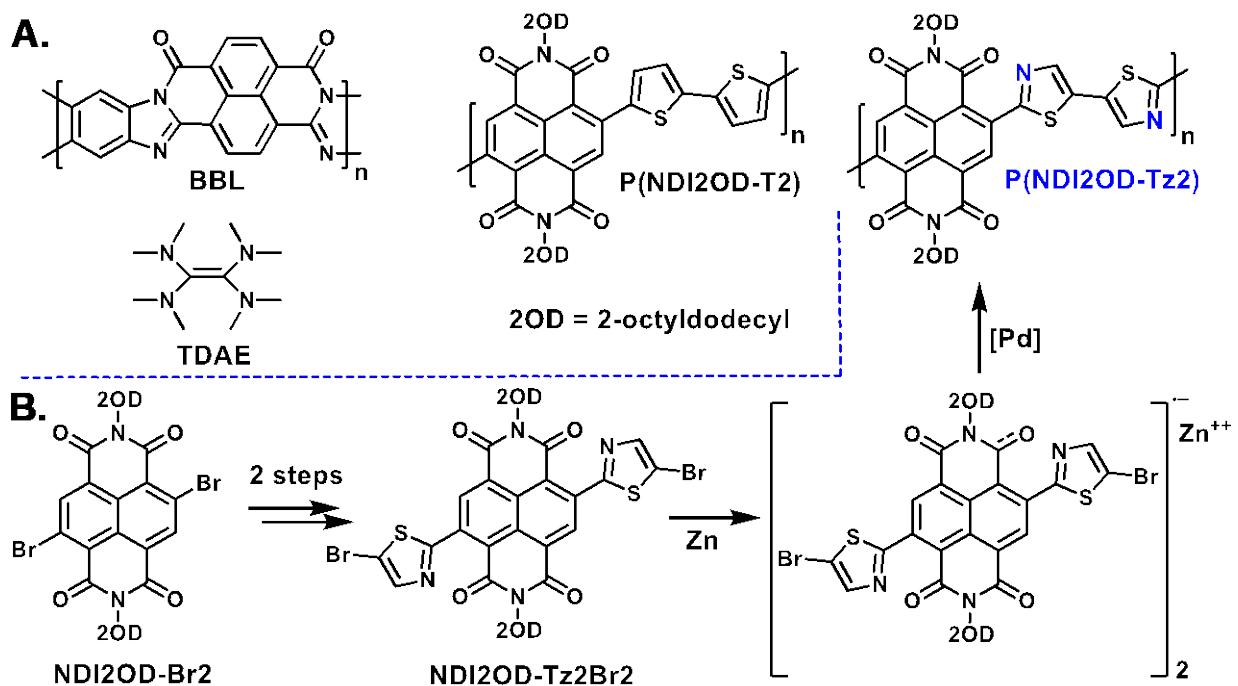


Figure 1. (A) Chemical structures of representative n-type polymers and the dopant TDAE. (B) Synthesis of P(NDI2OD-Tz2).

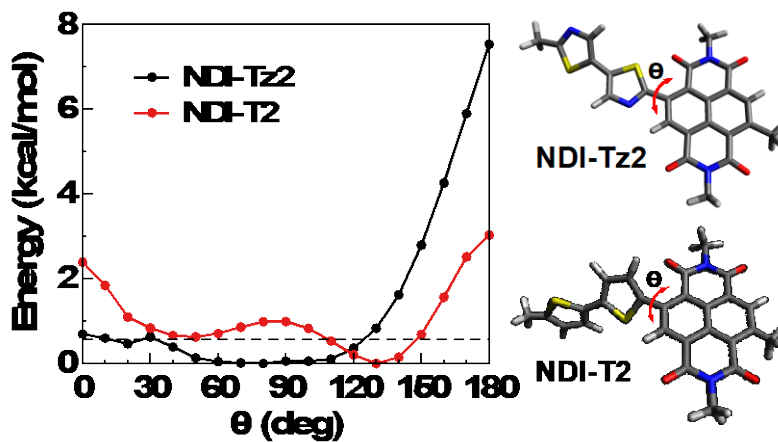


Figure 2. ω B97X-D/6-311G** relaxed potential energy- θ profiles for the indicated structures. The dashed line denotes $k_B T = \approx 0.6$ kcal mol⁻¹ at 298 K.

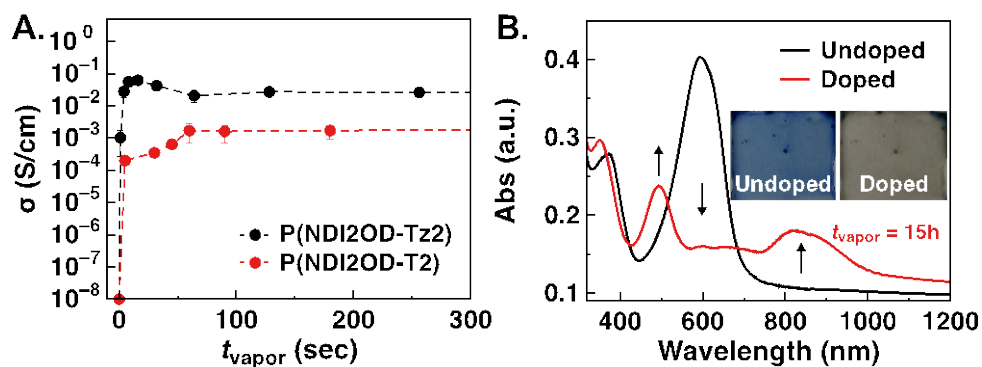


Figure 3. (A) Electrical conductivity of P(NDI2OD-Tz2) and P(NDI2OD-T2) films as a function of TDAE t_{vapor} . (B) Optical absorption spectra (inset, optical images) of P(NDI2OD-Tz2) films before and after TDAE doping ($t_{\text{vapor}} = 15$ h).

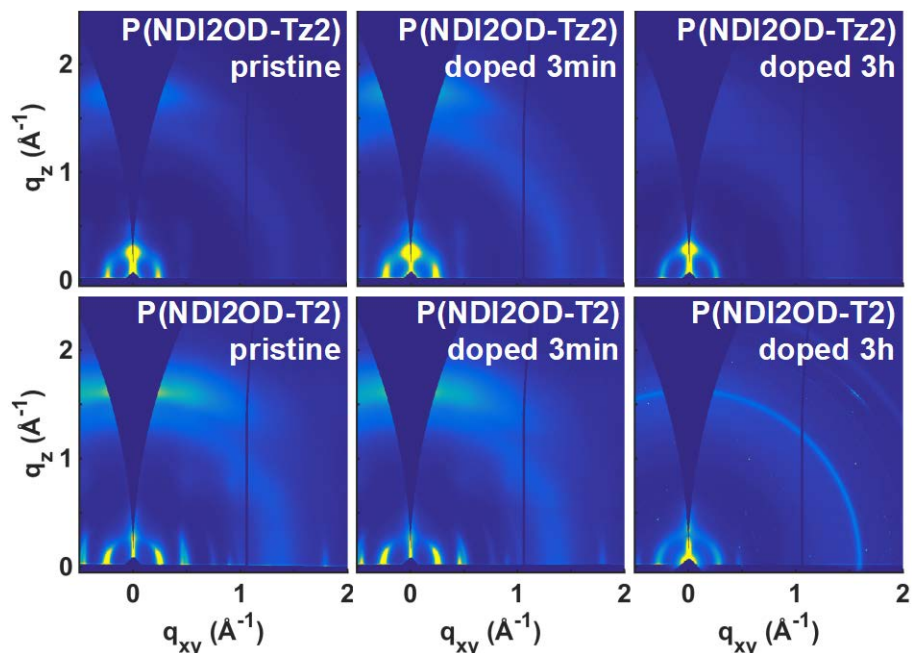


Figure 4. 2D GIWAXS patterns of pristine and doped P(NDI2OD-Tz2) and P(NDI2OD-T2) thin films.

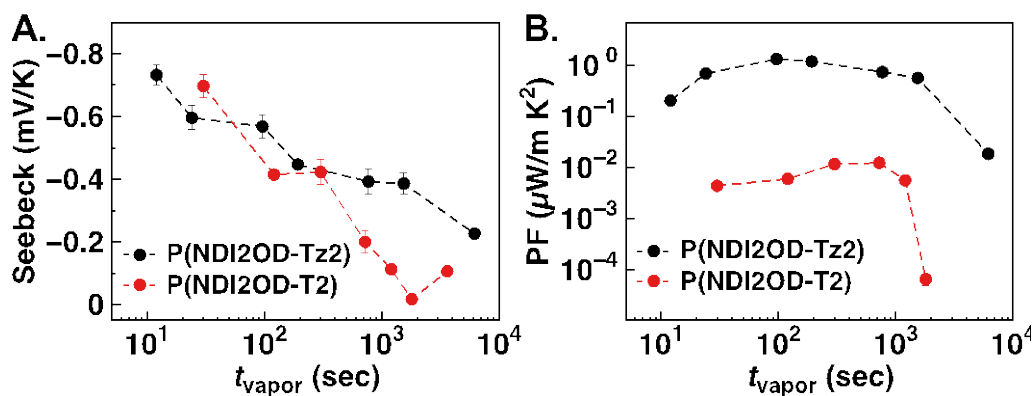


Figure 5. (A) Seebeck coefficient and (B) thermoelectric power factor (PF) as a function of TDAE exposure time for P(NDI2OD-Tz2) and P(NDI2OD-T2) films.

A novel naphthalenediimide-bithiazole n-type semiconducting polymer [P(NDI2OD-Tz2)] is synthesized and its structural, thin-film morphological, as well as charge transport and thermoelectric properties are compared to the parent naphthalenediimide-bithiophene polymer [P(NDI2OD-T2)]. The new n-type polymer has a greater backbone planarity and a reduced donor-acceptor character. When doped with a strong reducing agent, P(NDI2OD-Tz2) can reach electrical conductivity and thermoelectric power factor far superior to those of analogous P(NDI2OD-T2).

N-type organic thermoelectrics

Suhao Wang, Hengda Sun, Tim Erdmann, Gang Wang, Daniele Fazzi, Uwe Lappan, Yuttapoom Puttisong, Zhihua Chen, Magnus Berggren, Xavier Crispin, Anton Kiriy, Brigitte Voit, Tobin J. Marks,* Simone Fabiano,* Antonio Facchetti*

A chemically doped naphthalenediimide–bithiazole polymer for n-type organic thermoelectrics

